Oxygen Isotope Record of the 1997–1998 El Niño in Peruvian Sea Catfish (Galeichthys peruvianus) Otoliths

C. Fred T. Andrus – University of Georgia
Douglas E. Crowe – University of Georgia
Christopher S. Romanek – University of Georgia

Citation of published version:
Andrus, C., Crowe, D., Romanek, C. (2002): Oxygen Isotope Record of the 1997–1998 El Niño in Peruvian Sea Catfish (Galeichthys peruvianus) Otoliths. *Paleoceanography*, 17(4).
DOI: https://doi.org/10.1029/2001PA000652

Oxygen isotope record of the 1997–1998 El Niño in Peruvian sea catfish (*Galeichthys peruvianus*) otoliths

C. Fred T. Andrus, Douglas E. Crowe, and Christopher S. Romanek[1]
Department of Geology, University of Georgia, Athens, Georgia, USA

Received 2 May 2001; revised 9 January 2002; accepted 23 January 2002; published 11 October 2002.

[1] Sagittal otoliths of the Peruvian sea catfish *Galeichthys peruvianus* were collected from the north coast of Peru during and after the 1997–1998 El Niño. The otoliths were analyzed via laser microprobe and micromilling techniques for oxygen isotope composition through ontogeny to document their use as an El Niño-Southern Oscillation (ENSO) proxy. Results were compared to theoretical calculations for the $\delta^{18}O$ of otolith aragonite using measured sea surface temperatures (SST) and $\delta^{18}O$ values for local seawater assuming equilibrium oxygen isotope fractionation was achieved. All otoliths recorded the 1997–1998 El Niño event as well as seasonal temperature variations. These ENSO events were recorded in otolith aragonite as significant negative excursions in $\delta^{18}O$ that reflected the increased temperature of local marine waters. The combined otolith data were used to create a 10-year SST record, including ENSO events and local seasonal temperature variation, validating the use of otolith $\delta^{18}O$ as a temperature proxy. *INDEX TERMS:* 4522 Oceanography: Physical: El Niño; 1040 Geochemistry: Isotopic composition/chemistry; 4870 Oceanography: Biological and Chemical: Stable isotopes; 9355 Information Related to Geographic Region: Pacific Ocean; 9360 Information Related to Geographic Region: South America; *KEYWORDS:* El Niño, ENSO, otolith, stable isotopes, Peru, Galeichthys peruvianus

Citation: Andrus, C. F. T., D. E. Crowe, and C. S. Romanek, Oxygen isotope record of the 1997-1998 El Niño in Peruvian sea catfish (*Galeichthys peruvianus*) otoliths, *Paleoceanography*, *17*(4), 1053, doi:10.1029/2001PA000652, 2002.

1. Introduction

[2] Otoliths are incrementally precipitated aragonite structures found within the inner ear of teleost fish. Three pairs of otoliths (sagittae, lapillae, and asteriscii) are present in each fish. Sagittal otoliths are the largest and most studied of the three pairs and are the otoliths described in this paper. They are traditionally a rich source of fisheries biology data. Otolith growth increments, seen in thin section as alternating opaque and translucent bands in transmitted light (Figure 1), are used to determine season of birth, age at death, growth rate, and a number of other parameters relevant to fisheries stock management [*Secor et al.*, 1995]. The periodicity of increment formation must first be determined through control studies [*Beamish and McFarlane*, 1983], but annual (macroscopic) and daily (microscopic) bands are often observed in many species [*Campana and Neilson*, 1985; *Gauldie and Nelson*, 1990a].

[3] *Devereux* [1967] first demonstrated that otoliths are precipitated in or near oxygen isotope equilibrium with natural waters, and subsequent studies have refined the relationship between $\delta^{18}O$ values in otoliths and ambient waters through ontogeny [e.g., *Kalish*, 1991; *Patterson et al.*, 1993; *Thorrold et al.*, 1997]. These studies developed empirically derived equations [similar to *Grossman and Ku*, 1986] relating the $\delta^{18}O$ of aragonite to temperature, given a knowledge of the $\delta^{18}O$ of the water in which the fish lived.

[4] Otoliths are potentially valuable climate proxies. Otolith morphology is frequently taxon specific, thus even in the absence of other remains species identification is possible [*Gaemers*, 1984; *Wheeler and Jones*, 1989]. They are common worldwide in maritime archaeological sites, and are also found in sedimentary deposits as old as the Jurassic [*Patterson*, 1999]. Because otoliths are found over a wide geographic range, they offer insight into climatic conditions in areas that lack more traditional climate indicators, such as corals and ice cores. Of particular importance are otoliths in archaeological sites that date from preindustrial times, as they offer an opportunity to examine climate change that is not recorded in the historical literature.

[5] Incremental growth studies of otoliths from archaeological sites have been used for prehistoric fish population age profile reconstructions [*Casteel*, 1976; *Hales and Reitz*, 1992; *Van Neer et al.*, 1999] and season of capture determinations [*Van Neer et al.*, 1999; *Higham and Horn*, 2000]. Isotopic analysis of ancient otoliths has been used for paleoclimate reconstruction [*Patterson*, 1998, 1999; *Andrus et al.*, 1999; *Wurster and Patterson*, 2001]. In each case, modern populations of the same, or closely related species, were studied to provide a comparative baseline for the study of ancient otoliths.

[6] The data presented in this study indicate that *Galeichthys peruvianus* otoliths are robust proxies of ENSO conditions along the temperate coast of Peru. The value of this proxy is increased because this critical location lacks other

[1]Also at Savannah River Ecology Laboratory, Aiken, South Carolina, USA.

0883-8305/02/2001PA000652

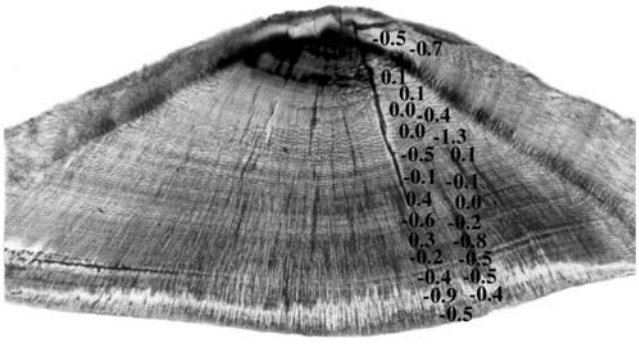

Figure 1. Transmitted light view of Otolith 99–2. Field of view is ~1 cm. Numbers are $\delta^{18}O$ in per mil relative to PDB.

suitable climate indicators [*Sandweiss et al.*, 1996]. Otoliths of many species, including *G. peruvianus*, are abundant and well preserved in archaeological sites ranging in age from the terminal Pleistocene to European contact [*Sandweiss et al.*, 1998; *Reitz*, 2001]. Paleotemperature records reconstructed from otoliths of this area will significantly strengthen our understanding of the origin and history of ENSO [*Rodbell et al.*, 1999].

2. Otolith Chemistry and Growth

[7] Otoliths function as electrical transducers aiding in acoustic perception and balance [*Morris and Kittleman*, 1967; *Fay*, 1980]. They are accretionary structures that grow incrementally from the endolymphatic fluid which, unlike other bodily fluids, closely resembles the natural waters in which the fish lives [*Degans et al.*, 1969; *Romanek and Gauldie*, 1996; *Gauldie and Romanek*, 1998]. Several studies have demonstrated that otoliths are precipitated in oxygen isotopic equilibrium with seawater [*Devereux*, 1967; *Kalish*, 1991; *Patterson et al.*, 1993; *Thorrold et al.*, 1997]. Because otoliths are accretionary structures, the $\delta^{18}O$ of the aragonite, from core to rim, preserves a continuous record of water temperature during the life of an individual fish.

[8] Most of the carbon in otolith aragonite is derived from bicarbonate dissolved in seawater, which is in isotopic equilibrium with atmospheric CO_2. The temperature dependence of carbon isotope fractionation in the aragonite-CO_2 system is negligible over the temperatures at which most fish live. A small proportion of the aragonite carbon is derived from metabolic CO_2, which is ^{13}C-depleted relative to seawater bicarbonate [*Thorrold et al.*, 1997]. Thus the utility of carbon isotopes in otolith aragonite in paleoclimate studies is limited (but see *Iacumin et al.* [1992] and *Thorrold et al.* [1997]). As such, oxygen isotopes have gained wider use in otolith paleoclimate research and will be the focus of this paper.

[9] Incremental growth of otoliths is manifest by concentric bands (Figure 1). Macroscopic bands, when viewed under transmitted light in thin section, alternate between opaque and translucent. Under higher magnification, these macroscopic bands are composed of groups of thinner bands that may represent daily growth [*Campana and Neilson*, 1985; *Gauldie and Nelson*, 1990b]. The width of macroscopic bands decreases in a roughly allometric pattern throughout ontogeny in most species. Where early growth bands are readily visible in most species, later growth near the outer margins of older fish can be difficult to discern at the macroscopic scale as band thickness decreases.

3. Species Description

[10] *G. peruvianus* otoliths were selected for analysis on the basis of several considerations: (1) The otoliths are comparatively large (~1 cm) and are amenable to microsampling by laser ablation and/or microdrilling. (2) The species does not migrate in response to El Niño or La Niña events, and thus continuously experiences temperature perturbations with time. (3) The species remains in shallow coastal waters year round in the Peruvian portion of its range, all of which is directly affected by ENSO. (4) The otoliths are common in Peruvian archaeological sites over a wide temporal range.

[11] *G. peruvianus*, known locally as "bagre", is described by *Lütken* [1874], *Kailola and Bussing* [1995], and *Froese and Pauly* [2001]. The published geographic range for the species is Mexico to Chile, but in field work for this study it was found to be common only to about 12°S, and was rarely captured further south than 16°S (Figure 2). In Peru, *G. peruvianus* was observed and captured only in marine environments. The steep shore face and microtidal conditions preclude the formation of brackish estuaries. The few, small braided rivers that cross the narrow coastal desert enter the Pacific Ocean abruptly and mix quickly with open ocean seawater.

4. Methods

[12] *G. peruvianus* were captured alive by local fisherman using small set nets from one-man reed boats near Pimentel (~6° 50'S.; July 1997) and Huanchaco (~8° 10'S.; July 1998, July 1999). The fish were dissected immediately after capture to remove the sagittal otoliths (see Figure 2 for map of collection sites). Water samples were collected for $\delta^{18}O$ analysis in July of 1998 and 1999 from the Pacific Ocean at Huanchaco.

[13] Sample preparation for microdrilling of carbonate and laser extraction of CO_2 was accomplished by bisecting the otolith across the longest axis of growth through the core with a low-speed diamond-wafering saw. A thick section was prepared from one of the otolith halves. The section was washed in distilled water, dried at room temperature, and briefly soaked in acetone and then pentane. All specimens were then immersed in 30% H_2O_2 for three hours to remove organic matrix and contamination, followed by degassing in a vacuum oven at 80°C for two days before microsampling. Thick sections for microdrill analysis were double polished until translucent and then were mounted on a standard petrographic slide.

[14] CO_2 was extracted from otoliths via laser ablation in an evacuated sample chamber following the technique described by *Andrus and Crowe* [2000]. Sampling was accomplished by ablation of a small (as small as ~90 μm

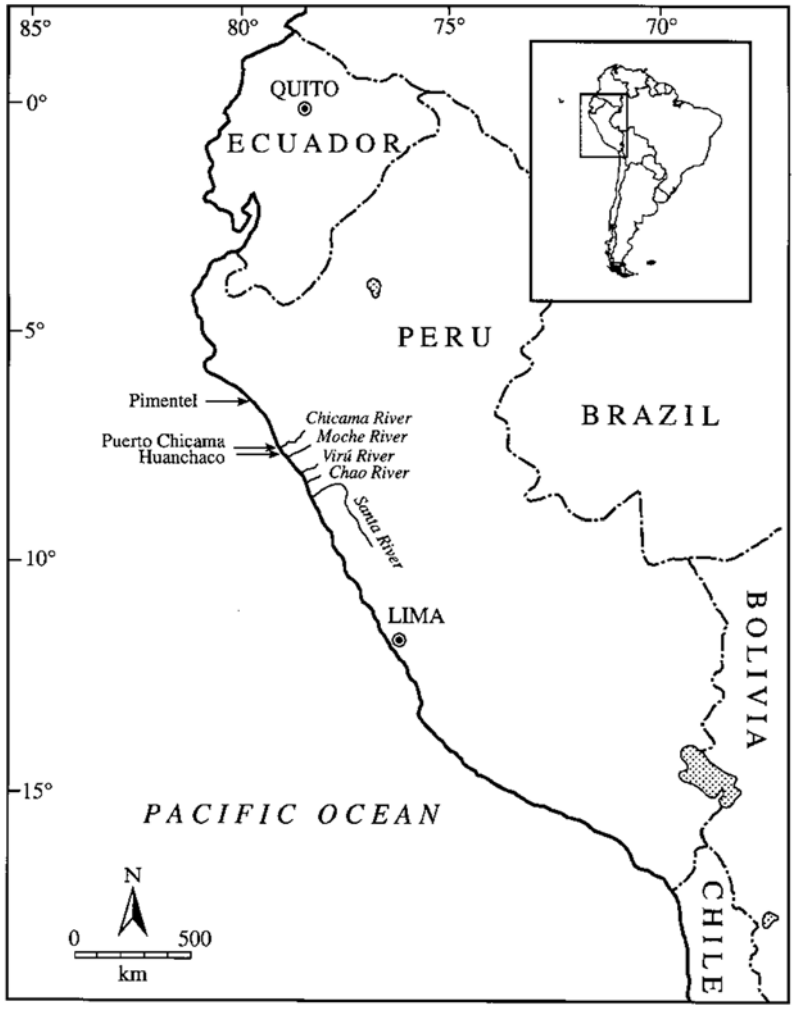

Figure 2. Map of collection area.

diameter, ~150 μm depth) sample volume with a Nd-YAG laser. At least one sample was ablated in each macroscopically visible growth band following ontogeny. Sequential sampling was conducted such that each laser pit was discrete and separate from the next. The laser was operated in Q-switched mode at 3.0 Khz. at a power setting of 14 watts. At 3.0 Khz. >90% CO_2 is produced, and fractionation between CO_2 and CO appears to be minimal [*Romanek et al.*, 1992].

[15] A typical analysis consisted of a brief laser pulse of 0.2–0.3 s. CO_2 generated via laser ablation was frozen into a liquid nitrogen cooled trap. Noncondensable gas pressure was measured and the noncondensable phases were pumped away. Liquid nitrogen was then replaced by a dry ice + ethanol bath, sublimating CO_2 for collection while retaining any water as a solid. The CO_2 was transferred on-line to a Finnigan MAT 252 gas-source isotope ratio mass spectrometer (IRMS) for measurement of $\delta^{13}C$ and $\delta^{18}O$. Results are reported relative to the PDB international standard using standard delta notation in ‰ units [*Craig*, 1957]. Working standards were processed each day in a similar fashion to estimate precision and accuracy. Data were corrected for laser fractionation by calibrating to a standard run with each sample otolith. Precision limits were better than ±0.2‰ for $\delta^{13}C$ (1σ), and ±0.23‰ (1σ) for $\delta^{18}O$ based on the Bancroft standard as reported in *Andrus and Crowe* [2000].

[16] Microdrilling was performed with a Merchantek EO micromill assembly. Drill transects were programmed from a digital video map of the otolith surface viewed in transmitted light. Macroscopic increment patterns were mapped and transects were drilled parallel to growth-lines, typically 150–200 μm deep. Sampling was conducted similar to *Dettman and Lohmann* [1995], where samples are drilled from the edge of the otolith inward, thus "whittling" away the carbonate at fine resolution. Powder was collected after milling and CO_2 was generated from the aragonite by phosphoric acid digestion [*Craig*, 1957]. Isotope ratios of this CO_2 were measured via IRMS. Daily working standards were analyzed to determine precision and accuracy of the method. Laboratory precision limits are better than ±0.1‰ (1σ) for $\delta^{13}C$ and $\delta^{18}O$ based on daily analysis of Harding Iceland spar standards [*Landis*, 1983].

[17] Water $\delta^{18}O$ analysis was conducted following the CO_2 equilibration method of *Socki et al.* [1992]. CO_2 gas

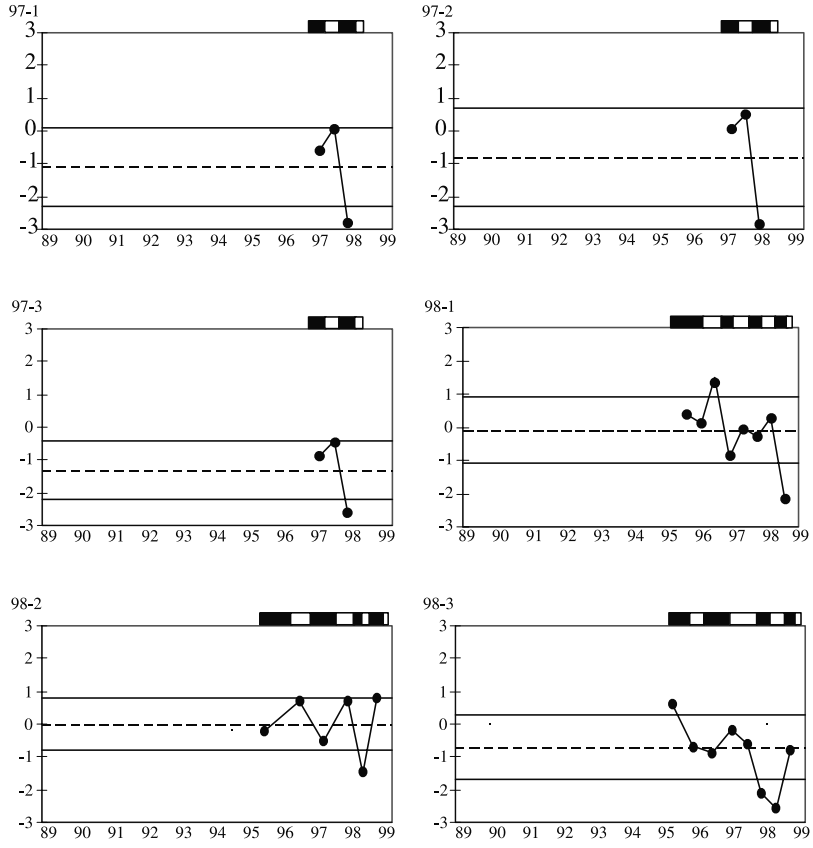

Figure 3. δ^{18}O as measured via laser microprobe. *Y* axis is δ^{18}O in per mil (PDB). *X* axis is time represented by macroscopic banding in the otolith. Left side is the core (birth), and right side is the time of capture. The first two digits in the sample label refer to the year of capture and the last digit is the otolith collection number. No data were collected from outermost growth of otolith 98−1. Dashed line is mean δ^{18}O value (see text), and solid lines are one standard deviation (1σ) from the mean. Bar at top of each panel represents increment type (black = opaque; white = translucent) as seen in transmitted light.

was measured on a Finnigan MAT Delta-E isotope ratio mass spectrometer. Results are reported relative to the SMOW international standard. Working standards were analyzed to monitor precision and accuracy. Precision limits were better than ±0.1‰ (1σ) for δ^{18}O based on daily analyses of a UGA working standard.

5. Results

[18] Optical examination of otolith thick sections revealed that each contained opaque and translucent bands in transmitted light. All otoliths, regardless of the year they were collected, were precipitating a narrow translucent band at the outer margin at the time of capture. Because they were all collected in July, it is assumed that this type of band corresponds to the austral winter and opaque bands to the austral summer. Therefore one opaque/translucent couplet represents one year of growth. Further, incremental growth and somatic growth rates appear related for *G. peruvianus* based on a positive correlation between the number of couplets and the measured size range of the sample fish (5 to 39 cm total length; 0.5 to 10.5 couplets).

[19] The results of all otolith laser analyses are plotted in Figure 3. The specimens (n = 3) captured in 1997 were collected at Pimentel, while all others were collected at Huanchaco in 1997 and 1998. All otolith data are plotted following ontogeny with core samples on the left. The otoliths from 1997 (Figure 3) are from young fish, and others in subsequent years are from older individuals. Microdrilled otolith sample results are plotted in Figure 4.

[20] In general, δ^{18}O profiles followed a roughly sinusoidal pattern. The mean amplitude of this oscillation was ~1‰, around an average δ^{18}O value of −0.1‰. Profile cyclicity was defined using the most extreme (highest or lowest) δ^{18}O values per increment (opaque or translucent); summary statistics (mean and standard deviation) were calculated using only these data to avoid bias toward periods of rapid growth. For example in Figure 3, otolith 98−3, the first, third, fourth, seventh and eighth points are used.

[21] There is a strong correlation between increment type (opaque or translucent in transmitted light) and δ^{18}O values, with the highest δ^{18}O values occurring in translucent increments, and the lowest values in opaque increments (see Figures 3 and 4). Assuming that bands are deposited

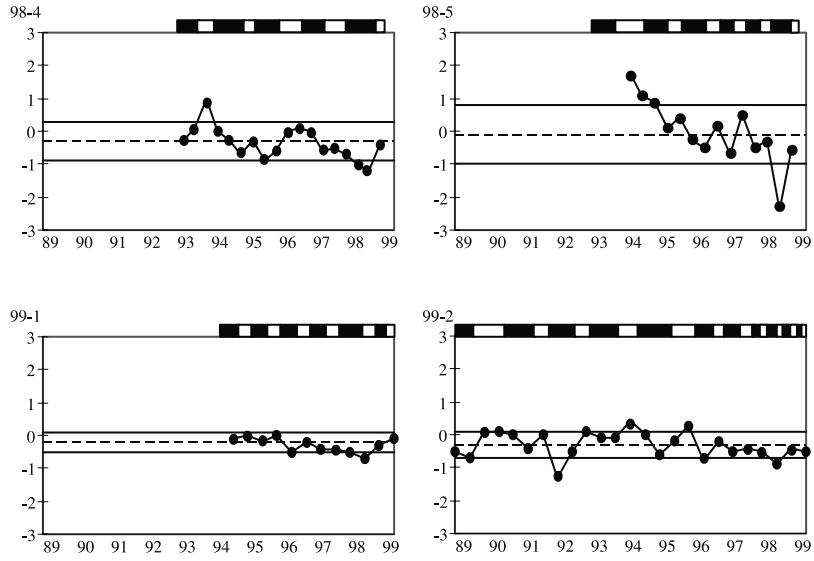

Figure 4. $\delta^{18}O$ as measured via micromill/phosphoric acid digestion technique. *Y* and *X* axes and lines are the same as in Figure 3.

seasonally, this means that the highest $\delta^{18}O$ values are associated with austral winter growth and the lowest $\delta^{18}O$ values are associated with austral summer growth. This observation is supported by the known relationship between temperature and $\delta^{18}O$ reported in the literature [e.g., *Grossman and Ku*, 1986].

[22] The $\delta^{18}O$ profiles differ depending on whether they were constructed using laser ablation or micromilling techniques and this is attributed to sequential sampling procedures and sampling scale. Estimates of sampling resolution are based on the volume of the carbonate sampled by laser or microdrill compared to the width of an increment. Increment width in an otolith decreases as the fish ages, with most rapid growth (widest bands) occurring in or near otolith cores when fish are young, and progressively slower growth (thinning bands) near the outer margin of the otolith in older fish (Figure 1). All else being equal, samples are of higher temporal resolution early in growth records where increments are wider and when accreting structures grow more quickly. Resolution diminishes with fish age as a result of the smaller increment width in geriatric increments.

[23] In the laser method, sample pits near the core were about one sixth to one third the width of an individual opaque or translucent band, thus the temporal sampling resolution was approximately 1–2 months of growth. Increment width near the otolith margin of old fish was roughly equivalent to the laser pit size, so temporal resolution was ~6 months.

[24] When sampling with the micromill, the transect width can be varied to match the width of an increment, thus the only limiting factor is the minimum amount of sample required to generate CO_2 for the IRMS analysis. Comparing the width of the transect necessary to produce enough carbonate for analysis to the increment width gives an estimate of temporal resolution. Toward the core of the otolith, an average of 2 transects were milled per increment, resulting in ~3 month resolution. Toward the margin of the otolith, generally only 1 transect was milled per increment, resulting in ~6 month resolution. In some very old fish, such as 99–2 (Figure 4), the outermost increments were so narrow that resolution was ~9 months. Unfortunately, some overlap in sampling was unavoidable with the micromill because the point of the drill bit is conical. The edge created after each pass was sloped toward the margin of the sample. When the drill bit made the next pass this material was included in the subsequent sample, so some homogenization occurred at a fine scale. The effect of this overlap was likely minimal in wide increments that were sampled in multiple transects but was more significant in narrow geriatric samples where increments were narrow. So although in some otoliths there were more micromill samples per increment than laser samples, each laser pit represented a discrete vertical sample volume through the section and thus a higher resolution temporal record.

[25] A further difficulty with micromilling is sample recovery. The micromill method requires the milled (powdered) aragonite to be removed from the sample surface manually and then transferred to the reaction vessel. Aragonite powder was lost during each stage of this process and thus the volume of the drilled sample was significantly greater than that from the laser pit where ~100% recovery was achieved. As a result of these sampling properties, the micromill data did not record the same extremes in $\delta^{18}O$ as the laser data.

6. Equilibrium Modeling

[26] A model was developed to predict the $\delta^{18}O$ of aragonite precipitated in equilibrium with seawater collected at Huanchaco (-0.5 ± 0.2‰ 1σ; n = 4) using the oxygen isotope/temperature equation of *Grossman and Ku* [1986] and the historical average monthly SST records from Puerto Chicama (8° S. Figure 5, top panel) for the period from January 1989 to February 1999 (Joint Institute for the Study of the Atmosphere and the Oceans (JISAO), World Wide

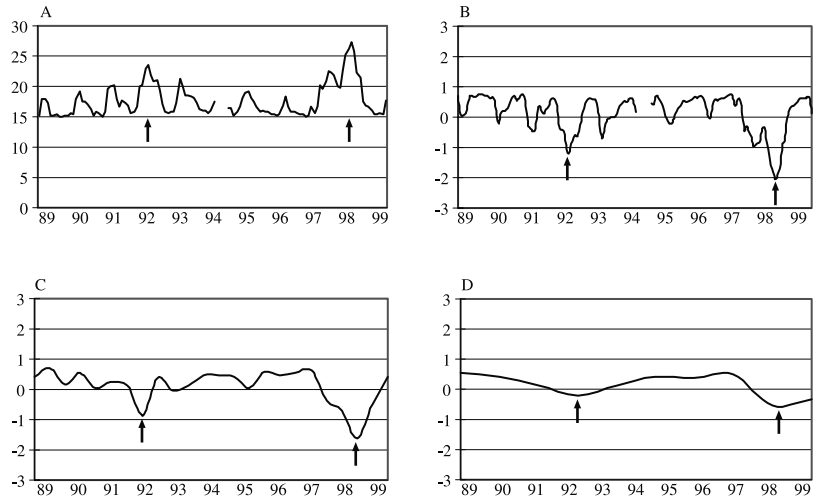

Figure 5. Models of $\delta^{18}O$ values for otolith aragonite assuming equilibrium fractionation following the *Grossman and Ku* [1986] relationship, using temperature data recorded at Puerto Chicama, January 1989 to February 1999 and the mean $\delta^{18}O$ value for seawater at Huanchaco (−0.5‰). (a) Average monthly SST data measured at Puerto Chicama from 1989–1999. (b) Model at a 1-month time average (gap represents a period in which no temperature measurements were reported). (c) A 5-month time average. (d) A 12-month time average. 1991–1992 and 1997–1998 El Niño events are noted on the plot with arrows.

Web database, Sea Surface Temperatures, Puerto Chicama, Peru, IGP, available at http://tao.atmos.washington.edu/data_sets/chicama_sst/, 2000). Using the model, a ~0.26‰ change in $\delta^{18}O$ is equivalent to a 1° C change in temperature following the *Grossman and Ku* [1986] relationship and assuming constant $\delta^{18}O_{water}$. The effect of temporal resolution was evaluated by averaging predicted $\delta^{18}O$ values at 2 through 12-month time intervals (1, 5, and 12-month resolutions are depicted in Figure 5). For example, the 12-month time average model was created by averaging the monthly predicted $\delta^{18}O$ values for each one-year period.

7. Discussion

[27] To define how accurately a proxy records ENSO conditions at a particular site local records must be evaluated within the context of a global phenomenon. The most widely accepted quantitative definitions refer to particular regions in the central Pacific. For example, *Trenberth* [1997] proposed a definition of ENSO for the Niño 3.4 region (5°N to 5°S, 170°W to 120°W) in which an El Niño event is defined by a +0.4° C deviation from a 5-month running mean of SST for at least 6 months. Such absolute and geographically limited measurements are not practical for use with most paleoclimate proxy data. Another definition, only applicable to the Peruvian coast north of 12°S latitude, was proposed by *Scientific Committee on Oceanic Research* (*SCOR*) [1983] in which El Niño is defined as a SST anomaly exceeding one standard deviation for at least four consecutive months measured at three out of five Peruvian coastal stations.

[28] In our analyses, the *SCOR* [1983] standard deviation-based measurement of ENSO conditions was used to identify El Niño events off the coast of Peru as negative excursions in the $\delta^{18}O$ (i.e. increased SST) in otolith carbonate records. The model of $\delta^{18}O$ for otolith aragonite from the period 1989–1999 shows two large negative excursions in $\delta^{18}O$ (Figure 5; marked by arrows). These excursions are evident at all time averages, although at 12 months, the 1991–1992 and 1997–1998 events become significantly attenuated. At the 5-month time average, both El Niño events are recorded as negative excursions in $\delta^{18}O$ greater than one standard deviation from the mean of most positive and negative $\delta^{18}O$ values per annual cycle (hereafter referred to as mean $\delta^{18}O$).

[29] All of the otolith profiles contained a negative excursion exceeding one standard deviation from the $\delta^{18}O$ mean during the 1997–1998 El Niño event (Figures 3 and 4). The incremental growth pattern of the otolith (opaque and translucent bands) permits independent determination of the portion of the otolith precipitated at the time of the 1997–1998 El Niño event, but care must be taken when interpreting these incremental growth patterns. *Meekan et al.* [1999] noted growth checks (periods of growth cessation) in Galápagos coral reef fish otoliths in response to the 1982–1983 El Niño event, but no such anomalous growth was noted in the catfish otoliths of this study. This may be due to the wide temperature tolerance of *G. peruvianus*.

[30] The progression of the El Niño temperature anomaly can be seen through time in the otoliths collected in different years. The otoliths 97–1, 97–2, and 97–3 (Figure 3) are from very young and small fish, and therefore the mean and standard deviation values are less constrained, but nonetheless the initial warming phase of the El Niño event is well-defined (right-most datum). Specimens 98–1 through 98–5 (Figures 3 and 4) recorded the complete 1997–1998 warming trend, while the otoliths 99–1 and 99–2 (Figure 4) recorded the entire warm phase of ENSO as well as

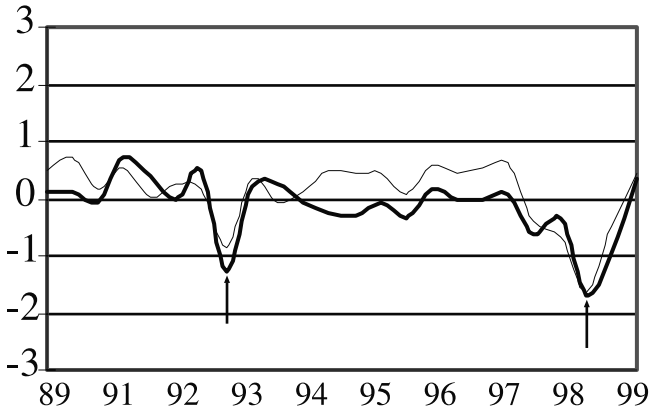

Figure 6. Composite of all otolith δ^{18}O values versus model results. *Y* axis is δ^{18}O in per mil (PDB). *X* axis is time from 1989–1999. Thick line is composite record from otoliths. Fine line is 5-month time average model data. Each data point in the composite was calculated based on the δ^{18}O values for time-equivalent packages of carbonate from all otolith samples using the macroscopic banding as a marker. 1991–1992 and 1997–1998 El Niño events are noted on the plot with arrows.

the subsequent cooling in 1998–1999. In otolith 99–2 (Figure 4), the 1991–1992 event is also detected. In this otolith, the 1991–1992 event appeared larger than the 1997–1998 event due to the decrease in increment width of the otolith in the geriatric individual.

[31] The correlation between the observed seasonal temperature fluctuations and the δ^{18}O records is striking given that SST data used in the model were measured from a stationary point, whereas the fish swam freely within local waters. Some fish may have entered regions of slightly different temperature conditions; as such otolith isotope profiles may differ slightly from the predictive model and other otoliths, even though each recorded the 1997–1998 El Niño event. Despite this expected variation, the otoliths all recorded seasonal SST variation similar to the measured SST's. The average seasonal temperature range derived from the otolith δ^{18}O values is $\sim$4°C and the measured range is 3.7°C.

[32] A composite δ^{18}O record of the last decade was created from the entire population of otolith profiles (Figure 6). The composite was constructed based on the known date of capture and the timing of macroscopic increment formation to identify carbonate deposited at synchronous time intervals. δ^{18}O values from each 6-month interval (opaque or translucent band) were averaged to create each data point in the composite. The 5-month resolution model and the 6-month otolith composite data most closely resemble one another (Figure 6). Both the 1991–1992 and 1997–1998 El Niño events are clearly evident as are more subtle seasonal temperature variations. The composite data are generally displaced by an average of -0.2‰ compared to the model data. This displacement is likely a result of the fish living in shallower coastal waters relative to the Puerto Chicama SST data source several kilometers away.

8. Conclusions

[33] Based on these analyses, it may be concluded that otoliths are valid proxies of SST's and therefore ENSO conditions. In areas such as coastal Peru where no other quantifiable records are available from other proxies (e.g. corals), otoliths offer a viable method of measuring former seasonal and inter-annual temperature variations. Insights into past seasonal and inter-annual SST variation in this area are needed to clarify related paleoclimate data and models [*Bush*, 2001]. Paleo-ENSO frequency determination may be enhanced using archaeological otoliths because they are often from individuals which lived longer than modern fish, due to lower fishing pressure in the past; they may record over 25 years of continuous climate history [*Andrus et al.*, 1999].

[34] **Acknowledgments.** This research was funded in part by grants from the Geological Society of America (CFTA), Explorer's Club International (CFTA), NSF grant ATM-0082213 (DEC), and DOE financial assistance award DE-FC09-96SR18546 to the Savannah River Ecology Laboratory through the UGA Research Foundation (CSR). We wish to thank Daniel Sandweiss and Elizabeth Reitz for assistance and advice throughout this project. Sally Walker, David Wenner, and Ervan Garrison all contributed thoughtful criticism of this research. We are grateful to Bill McCLain of the University of Georgia Stable Isotope Laboratory for help with the stable isotope analyses. We appreciate the assistance in the field provided by Miguel Cornejo of the University of Trujillo, Peru, and Tom Wake (UCLA) for providing laboratory space for dissection in Huanchaco, Peru.

References

Andrus, C. F. T., and D. E. Crowe, Geochemical analyses of *Crassostrea virginica* as a method to determine season of capture, *J. Archaeol. Sci.*, *27*, 33–42, 2000.

Andrus, C. F. T., D. E. Crowe, and D. S. Sandweiss, Geochemical evidence of mid-Holocene ENSO variation derived from otoliths, *Eos Trans AGU*, *80*(46), Fall Meet. Suppl., F575, 1999.

Beamish, R. J., and G. A. McFarlane, The forgotten requirements for age validation in fisheries biology, *Trans. Am. Fish. Soc.*, *112*, 735–743, 1983.

Bush, A. B. G., Pacific sea surface temperature forcing dominates orbital forcing of the early Holocene monsoon, *Quat. Res.*, *55*, 25–32, 2001.

Campana, S. E., and J. D. Neilson, Microstructure of fish otoliths, *Can. J. Fish. Aquat. Sci.*, *42*, 1014–1032, 1985.

Casteel, R. W., *Fish Remains in Archaeology and Paleo-environmental Studies*, Academic, San Diego, Calif., 1976.

Craig, H., Isotopic standards for carbon and oxygen and correction factors for mass-spectrometric analysis of carbon dioxide, *Geochim. Cosmochim. Acta*, *12*, 133–149, 1957.

Degans, E. T., W. G. Deuser, and R. L. Haedrich, Molecular structure and composition of fish otoliths, *Mar. Biol.*, *2*, 105–113, 1969.

Dettman, D. L., and K. C. Lohmann, Microsampling carbonates for stable isotope and minor element analysis: Physical separation of samples on a 20 micrometer scale, *J. Sediment. Res.*, *65*, 566–569, 1995.

Devereux, I., Temperature measurements from oxygen isotope ratios of fish otoliths, *Science*, *155*, 1684–1685, 1967.

Fay, R. R., The goldfish ear codes the axis of acoustic particle motion in three dimensions, *Science.*, *225*, 951–963, 1980.

Froese, R., and D. Pauly (Eds.), *Fishbase*, Int. Cent. for Living Aquat. Resour. Manage., Los Baños, Laguna, Philippines, 2 March 2001. (Available at http://www.fishbase.org)

Gaemers, P. A., Taxonomic position of the cichlidae (Pisces, Perciformes) as demonstrated by the morphology of their otoliths, *Neth. J. Zool.*, *34*, 566–595, 1984.

Gauldie, R. W., and D. G. A. Nelson, Interaction between crystal ultrastructure and microincrement layers in fish otoliths, *Compar. Biochem Physiol.*, *974*, 449–459, 1990a.

Gauldie, R. W., and D. G. A. Nelson, Otolith

growth in fishes, *Compar. Biochem Physiol.*, *97*, 119–135, 1990b.

Gauldie, R. W., and C. S. Romanek, Orange roughly otolith growth rates: A direct experimental test of the Romanek-Gauldie otolith growth model, *Compar. Biochem. Physiol.*, *120*, 649–653, 1998.

Grossman, E. L., and T. L. Ku, Oxygen and carbon isotopic fractionation in biogenic aragonite, *Chem. Geol.*, *59*, 59–74, 1986.

Hales, L. S., and E. J. Reitz, Historical changes in age and growth of Atlantic Croaker, *Micropogonius undulatus* (Perciformes: Sciaenidae), *J. Archaeol. Sci.*, *19*, 73–99, 1992.

Higham, T. F. G., and P. L. Horn, Seasonal dating using fish otoliths: Results from the Shag River Mouth site, New Zealand, *J. Archaeol. Sci.*, *27*, 439–448, 2000.

Iacumin, P., G. Bianucci, and A. Longinelli, Oxygen and carbon isotopic content of fish otoliths, *Mar. Biol.*, *113*, 537–542, 1992.

Kailola, A. N., and W. A. Bussing, Ariidae, *Bagres marinos*, in *Guia FAO para identification de especies para lo fines de la pesca, Pacifico centro-oriental*, edited by W. Fischer et al., pp. 860–886, Food and Agric. Organ., Rome, 1995.

Kalish, J. M., C-13 and O-18 isotopic disequilibria in fish otoliths: Metabolic and kinetic effects, *Mar. Ecol. Prog. Ser.*, *75*, 191–203, 1991.

Landis, G. P., Harding Iceland spar: A new $\delta^{18}O$ – $\delta^{13}C$ carbonate standard for hydrothermal minerals, *Isotope Geosci.*, *1*, 91–94, 1983.

Lütken, C. F., Ichthyographike Bidrag, II, Nye eller mindre vel kjendte Malleformer fra forskjellige Verdensdele, Vidensk, *Medd. Naturh. Foren. Köbenhavn*, 190–220, 1874.

Meekan, M. G., G. M. Wellington, and L. Axe, El Niño-Southern Oscillation events produce checks in the otoliths of coral reef fishes in the Galápagos Archipelago, *Bull. Mar. Sci.*, *64*, 383–390, 1999.

Morris, R. W., and L. R. Kittleman, Piezoelectric property of otoliths, *Science*, *158*, 368–370, 1967.

Patterson, W. P., North American continental seasonality during the last millennium: High-resolution analysis of sagittal otoliths, *Palaeogeogr. Palaeoclimatol. Palaeoecol.*, *38*, 271–303, 1998.

Patterson, W. P., Oldest isotopically characterized fish otoliths provide insight to Jurassic continental climate of Europe, *Geology*, *27*, 199–202, 1999.

Patterson, W. P., G. R. Smith, K. C. Lohman, Continental paleothermometry and seasonality using the isotopic composition of aragonitic otoliths of freshwater fishes, in *Climate Change in Continental Isotopic Records, Geophys. Monogr. Ser.*, vol. 78, edited by P. K. Swart et al., pp. 191–202, AGU, Washington, D. C., 1993.

Reitz, E. J., Fishing in Peru between 10,000 and 3750 B.P., *Int. J. Osteoarch.*, *11*, 163–171, 2001.

Rodbell, D. T., G. O. Seltzer, D. M. Anderson, M. A. Abbott, D. B. Enfield, and J. Newman, An ~15,000-year record of El Niño-driven alluviation in southwestern Ecuador, *Science*, *283*, 516–520, 1999.

Romanek, C. S., and R. W. Gauldie, A predictive model of otolith growth in fish based on the chemistry of the endolymph, *Compar. Biochem. Physiol.*, *114*, 71–79, 1996.

Romanek, C. S., E. K. Gibson Jr., and S. A. Socki, Gas speciation and ^{13}C and ^{18}O ratios of gasses generated by laser sampling of carbonate, *Geol. Soc. Am. Abstr. Prog.*, *24*, 216–217, 1992.

Sandweiss, D. H., J. B. Richardson III, E. J. Reitz, H. B. Rollins, and K. A. Maasch, Geoarchaeological evidence from Peru for a 5000 years BP onset of El Niño, *Science*, *273*, 1531–1533, 1996.

Sandweiss, D. H., H. McInnis, R. L. Burger, A. Cano, B. Ojeda, R. Paredes, M. Sandweiss, and M. D. Glasscock, Quebrada Jaguay: Early South American maritime adaptations, *Science*, *281*, 1830–1832, 1998.

Scientific Committee on Oceanic Research (SCOR), Prediction of El Niño, *SCOR WG 55*, pp. 47–51, Secretariat, Dep. of Earth and Planet. Sci., Johns Hopkins Univ., Baltimore, Md., 1983.

Secor, D. H., A. Henderson-Arzapalo, and P. M. Piccoli, Can otolith microchemistry chart patterns of migration and habitat utilization in anadromous fishes?, *J. Exp. Mar. Biol. Ecol.*, *192*, 15–33, 1995.

Socki, R. A., H. R. Karlesson, and E. K. Gibson, Extraction technique for the determination of oxygen-18 in water using preevacuated glass vials, *Anal. Chem.*, *64*, 829–831, 1992.

Thorrold, S. R., S. E. Campana, C. M. Jones, and P. K. Swart, Factors determining $\delta^{13}C$ and $\delta^{18}O$ fractionation in aragonitic otoliths of marine fish, *Geochim. Cosmochim. Acta*, *61*, 2909–2919, 1997.

Trenberth, K. E., The definition of El Niño, *Bull. Am. Meteorol. Soc.*, *78*, 2771–2777, 1997.

Van Neer, W., L. Löugas, and A. D. Rijnsdorp, Reconstructing age distribution, season of capture and growth rate of fish from archaeological sites based on otoliths and vertebrae, *Int. J. Osteoarcheol.*, *9*, 116–130, 1999.

Wheeler, A., and A. K. G. Jones, *Fishes*, Cambridge Manuals in Archaeology, Cambridge Univ. Press, New York, 1989.

Wurster, C. M., and W. P. Patterson, Late Holocene climate change for the eastern interior United States: Evidence from high-resolution sagittal otolith stable isotope ratios of oxygen, *Palaeogeogr. Palaeoclimatol. Palaeoecol.*, *170*, 81–100, 2001.

C. F. T. Andrus, D. E. Crowe, and C. S. Romanek, Department of Geology, University of Georgia, Athens, GA 30602, USA. (andrus@gly.uga.edu)